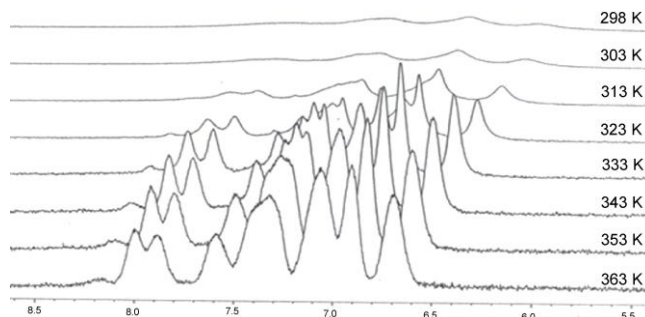
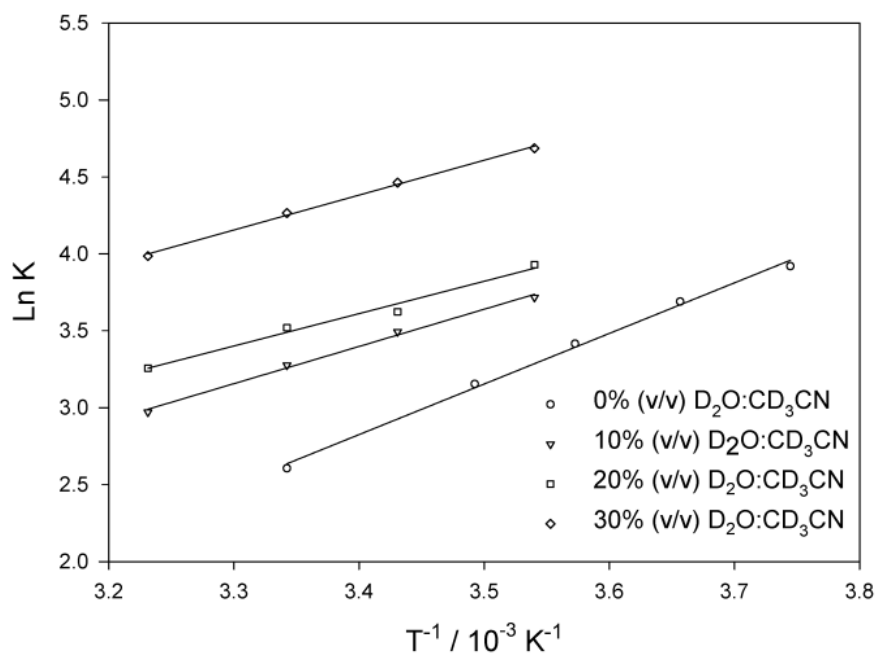


## Supporting Information

Izak A Kotzé,<sup>†</sup> Wilhelmus J Gerber,<sup>†</sup> Yu-Shan Wu<sup>†</sup> and Klaus R Koch<sup>†\*</sup>



**Figure S1.**  $^1\text{H}$  NMR (400 MHz) spectra of  $[\text{Pt}^{\text{II}}(1,10\text{-phenanthroline})(N,N\text{-di}(2\text{-hydroxyethyl})\text{-}N'\text{-benzoylthiourea})]\text{Cl}$  as in  $\text{D}_2\text{O}$  a function of temperature.<sup>14</sup> Note the extremely broad featureless NMR spectrum at 298 K, as well as the systematic de-shielding and sharpening of  $^1\text{H}$  peaks as the temperature increases.



**Figure S2.** Van't Hoff Plots of the dimerization of  $[\text{Pt}^{\text{II}}(\text{phen})(L^1\text{-}S,O)]^+$  in solutions 0-30% (v/v)  $\text{D}_2\text{O}:\text{CD}_3\text{CN}$ . The good linear fit obtained with the Van't Hoff equation is further validation for the self-association of  $[\text{Pt}^{\text{II}}(\text{phen})(L^1\text{-}S,O)]^+$  to form dimer aggregates in solution.

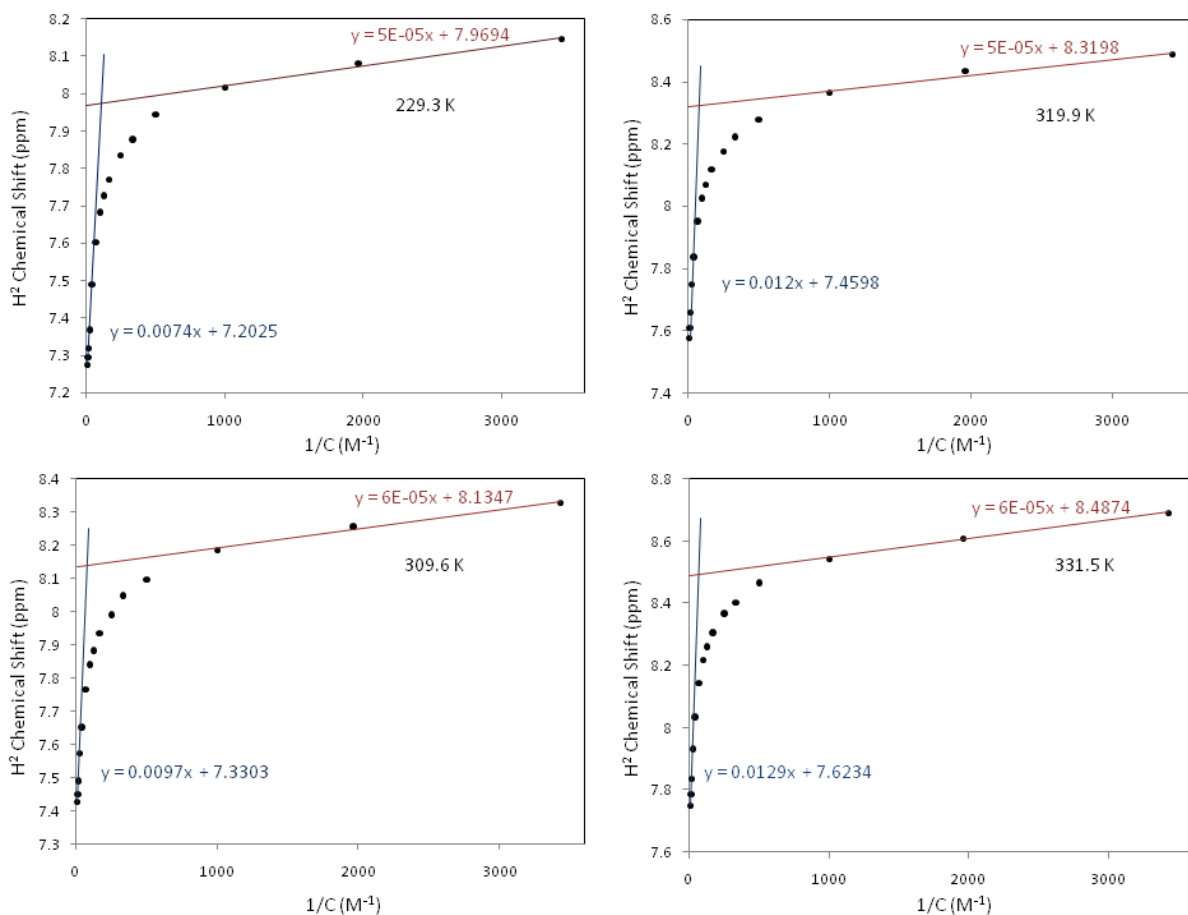


**Fig. S3.** The observed  $^1H$  chemical shift dependence of  $H^2$  at temperatures 299.3 - 331.5 K plotted against  $1/[M]_T$ , where  $[M]_T = \text{Total } [Pt^{II}(\text{phen})(L^1-S,O)]Cl$  concentration in  $D_2O$ .

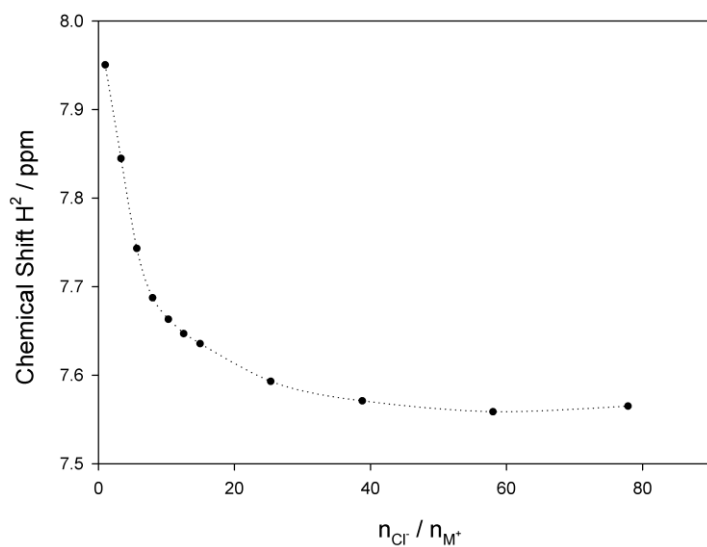


**Figure S4.** Variation of  $\delta_{\text{obs}}(H^2)$  as a function of increasing  $Cl^-$  concentration (as the  $Cl^-$  : cation ( $[Pt^{II}(\text{phen})(L^1-S,O)]^+$ ) ratio,  $n_{Cl^-} / n_{M^+}$ ) for a total  $[Pt^{II}(\text{phen})(L^1-S,O)]Cl$  concentration  $[Z] = 4.50$  mM; Precipitation occurs at a final  $Cl^-$  concentration of 346.7 mM.



**Figure S5.** TEM image of  $[\text{Pt}^{\text{II}}(2,2'\text{-bipyridyl})(N,N\text{-di}(2\text{-hydroxyethyl})\text{-}N'\text{-benzoylthiourea})]\text{Cl}$  prepared from water and stained with uranyl acetate at a 73000 X magnification.<sup>14</sup>

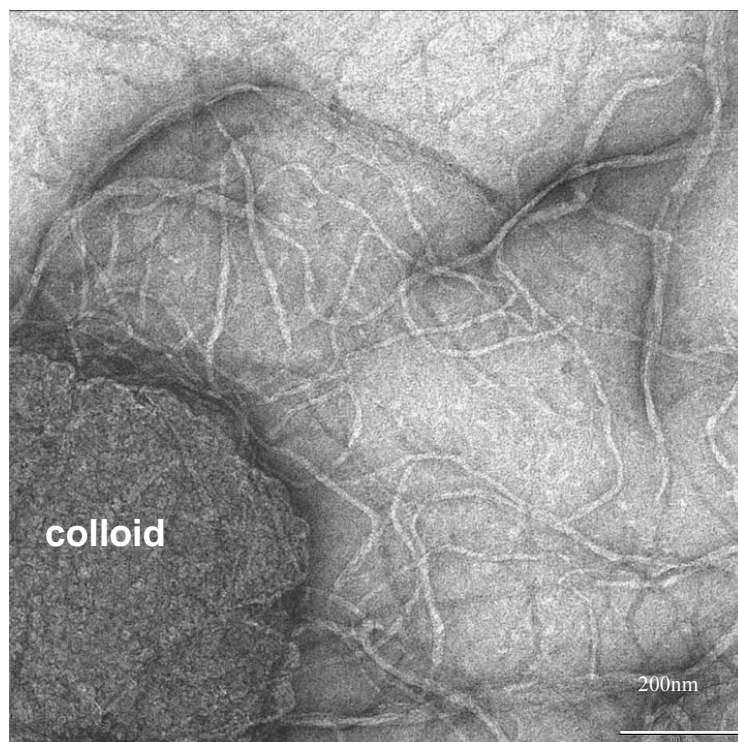


**Figure S6.** TEM images of  $[\text{Pt}^{\text{II}}(\text{phen})(L^1\text{-}S,O)]\text{Cl}$  in water showing the presence of micron-size colloid particles in aged solutions (>7 days).

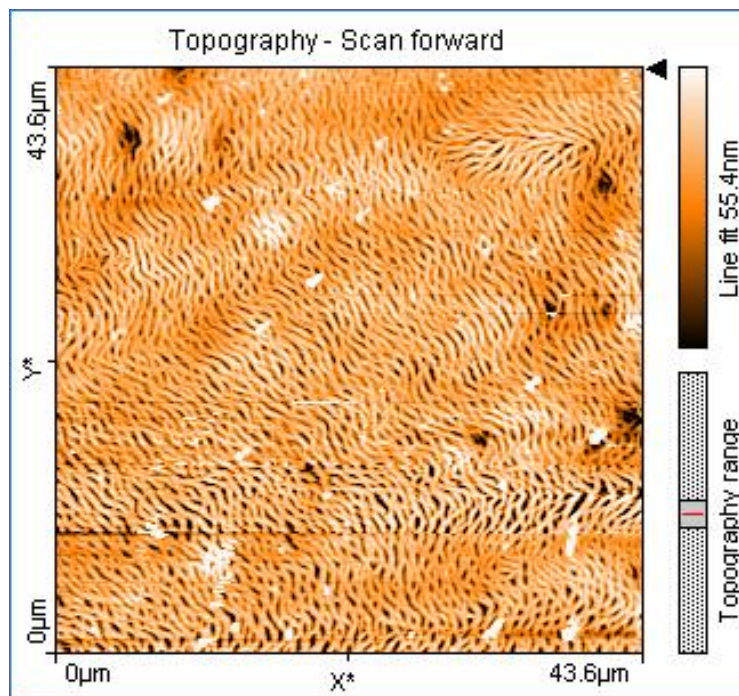


**Figure S7.** Atomic Force Microscopy (AFM) image of a spin-dried droplet of  $[\text{Pt}^{\text{II}}(\text{phen})(\text{L}^1\text{-S},\text{O})]\text{Cl}$  in acetonitrile on a silicon oxide disk.

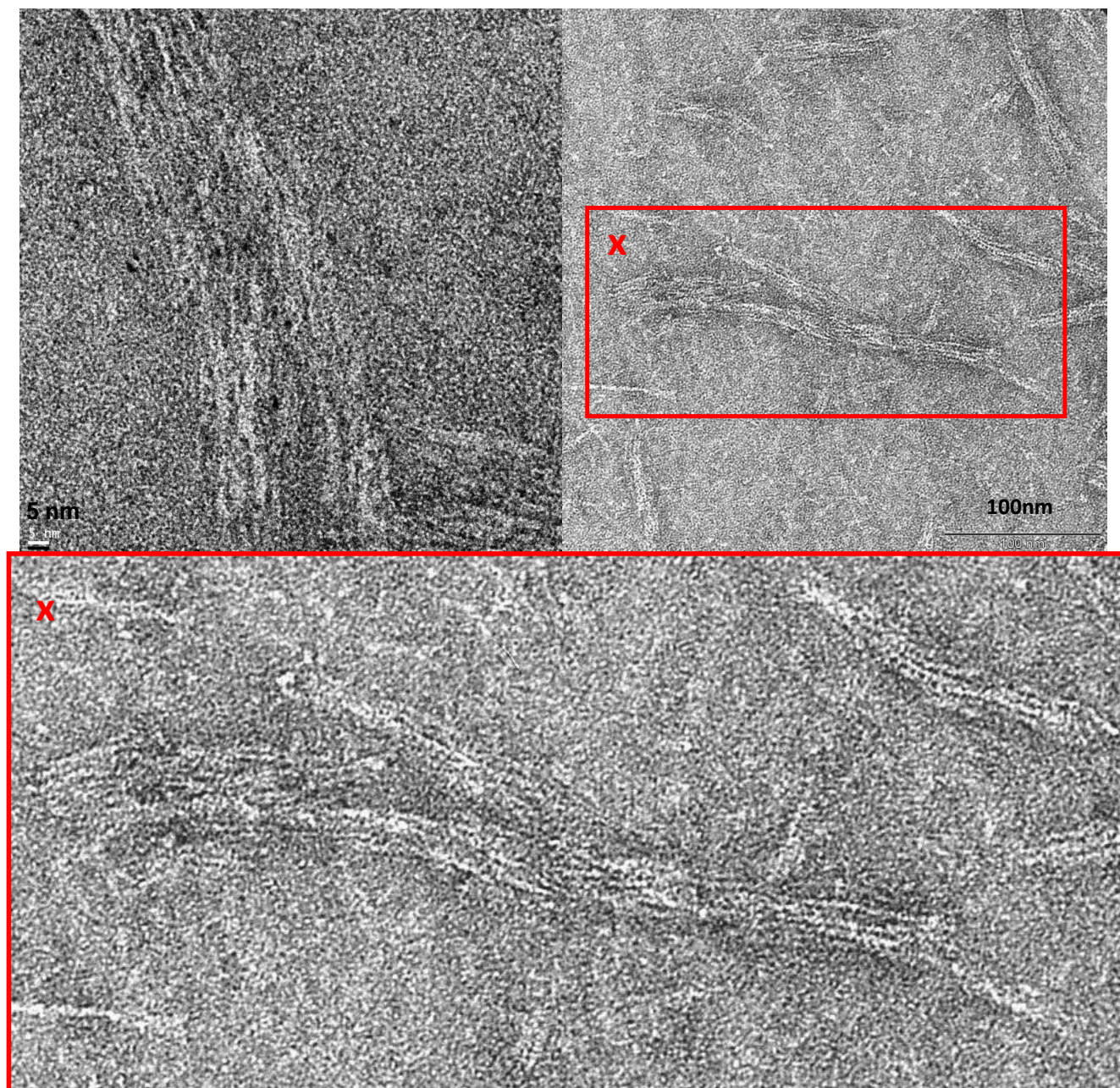


**Figure S8.** TEM images prepared from a freshly diluted sample of  $[\text{Pt}^{\text{II}}(\text{phen})(\text{L}^1\text{-S},\text{O})]\text{Cl}$  water showing the agglomerated ‘strands’ arise from the secondary structure of the nano-sizes aggregates.

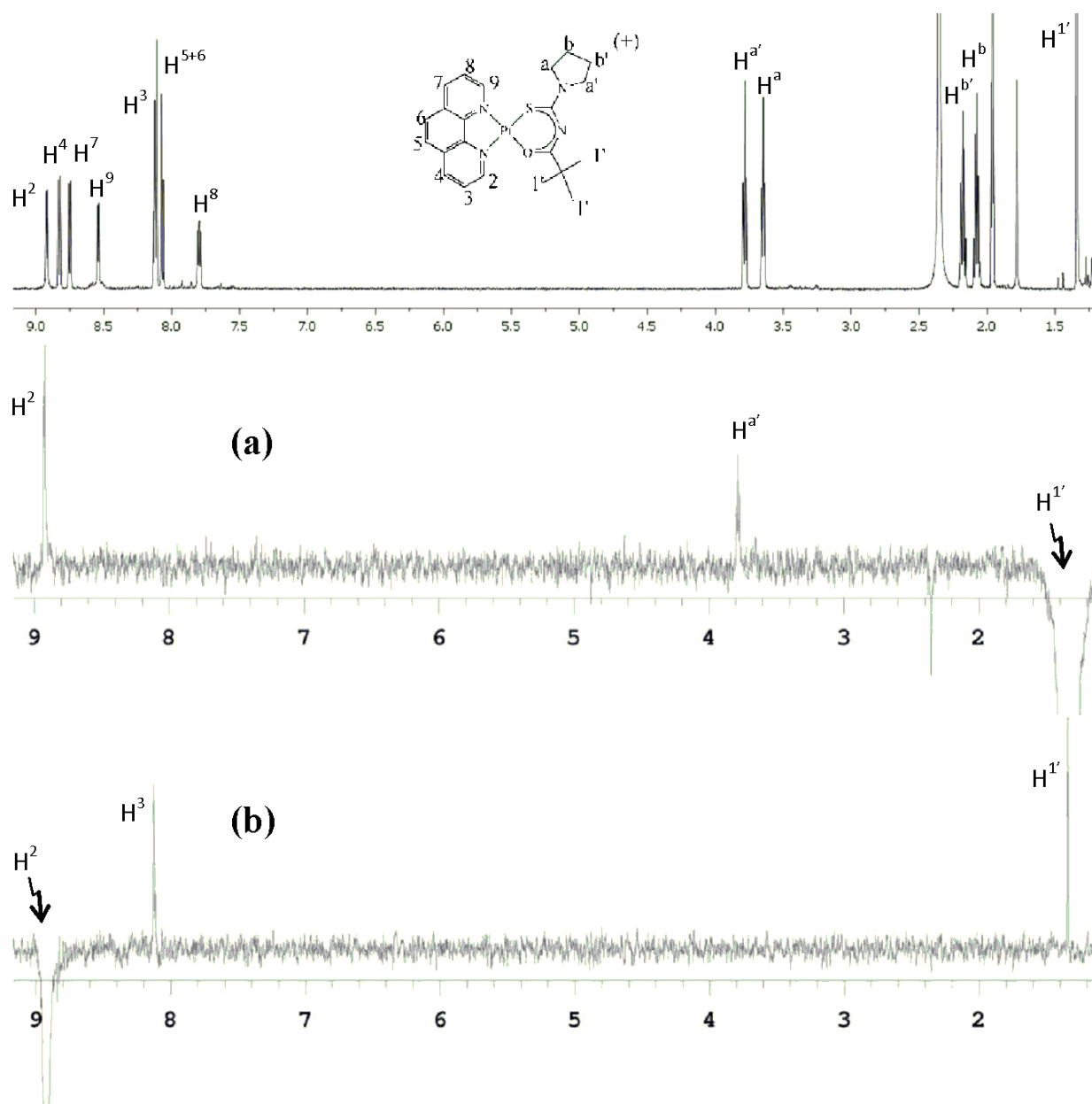


**Figure S9.**  $^1\text{H}$  NMR signal NOE enhancements in a 1D gNOESY experiment upon the irradiation of (a) the  $\text{H}^{1'}$  and (b)  $\text{H}^2$  protons of  $[\text{Pt}^{\text{II}}(\text{phen})(\text{L}^1\text{-S},\text{O})]\text{Cl}$  respectively. This confirms the assignment of the diimine protons  $\text{H}^2$  and  $\text{H}^9$  unambiguously.

**Table S1.** The calculated ‘monomer’ ( $\delta_m$  of  $[\text{Pt}^{\text{II}}(\text{phen})(\text{L}^1\text{-S},\text{O})]^+$ ) and dimer ( $\delta_d$  of  $\{[\text{Pt}^{\text{II}}(\text{phen})(\text{L}^1\text{-S},\text{O})]^+\}_2$ ) chemical shifts in acetonitrile-water mixtures of 10-30% (v/v)  $\text{D}_2\text{O}:\text{CD}_3\text{CN}$  using the  $(2[\text{Pt}^{\text{II}}(\text{phen})(\text{L}^1\text{-S},\text{O})]^+ \rightleftharpoons \{[\text{Pt}^{\text{II}}(\text{phen})(\text{L}^1\text{-S},\text{O})]^+\}_2)$  model. The error reflects the differences between the observed and calculated ( $\delta_m/\delta_d$   $^1\text{H}$  shifts of  $\text{H}^2$ )

Percentage (v/v) $\text{D}_2\text{O}:\text{CD}_3\text{CN}$	Temperature (K)	$\delta_m$ (ppm)	error (+-)	$\delta_d$ (ppm)	error (+-)
10	309.6	9.300	0.004	8.118	0.053
	299.3	9.292	0.006	8.123	0.064
	291.6	9.285	0.009	8.105	0.076
	282.6	9.273	0.015	8.087	0.099
20	309.6	9.281	0.006	8.195	0.067
	299.3	9.275	0.007	8.192	0.061
	291.6	9.269	0.023	8.098	0.145
	282.6	9.262	0.02	8.195	0.113
30	309.6	9.264	0.009	8.293	0.053
	299.3	9.26	0.01	8.281	0.048
	291.6	9.253	0.014	8.260	0.055
	282.6	9.246	0.017	8.252	0.054

**Table S2.** Variation of  $\delta_{\text{obs}}(\text{H}^2)$  and  $D_{\text{obs}}$  of a 4.5 mM  $[\text{Pt}^{\text{II}}(\text{phen})(\text{L}^1\text{-S},\text{O})]\text{Cl}$  solution as a function of NaCl concentration with the calculated hydrodynamic radii ( $r_{\text{H}}$ ), volumes ( $V_{\text{H}}$ ) and aggregation numbers ( $N$ ).

Mole Ratio	$\delta_{\text{obs}}(\text{H}^2)$	Mole Ratio	$D$	$r_{\text{H}}$	$V_{\text{H}}$	$N$
$n_{\text{Cl}^-}:n_{\text{M}^+}$	(ppm)	$n_{\text{Cl}^-}:n_{\text{M}^+}$	( $10^{-10}\text{m}^2\cdot\text{s}^{-1}$ )	(Å)	(Å <sup>3</sup> )	( $V_{\text{H}}/V_{\text{H}}^0$ )
1	7.95	1	1.70	11.9	7060	7.0
3.32	7.84	2.33	1.43	14.2	11904	11.8
5.65	7.74	4.66	1.23	16.5	18660	18.5
7.97	7.69	8.15	1.05	19.4	30503	30.3
10.30	7.69	10.8	0.96	21.1	39221	39.0
12.53	7.65	18.3	0.80	25.4	68242	67.8
14.94	7.64	29.1	0.69	29.5	107824	107
25.35	7.59	43.0	0.63	32.3	140543	140
38.80	7.57	50.6	0.61	33.4	155640	155
58.02	7.56	61.4	0.58	34.9	177484	176
77.88	7.57					

**Table S3.**  $^1\text{H}$   $\delta_{\text{obs}}(\text{H}^2)$  and  $D_{\text{obs}}$  dependence of  $[\text{Pt}^{\text{II}}(\text{phen})(\text{L}^1\text{-S},\text{O})]\text{Cl}$  (4.5 mM) on NaCl concentration with corresponding hydrodynamic radii ( $r_{\text{H}}$ ), volumes ( $V_{\text{H}}$ ) and aggregation numbers ( $N$ ).

$[\text{M}]_{\text{T}}^{-1}$ ( $\text{M}^{-1}$ )	$\delta_{\text{obs}}(\text{H}^2)$ (ppm)			
	299.3 K	309.6 K	319.9K	331.5 K
9.8141	7.275	7.427	7.577	7.750
12.582	7.295	7.451	7.611	7.786
16.691	7.318	7.491	7.658	7.837
25.021	7.368	7.574	7.749	7.932
40.004	7.489	7.652	7.837	8.036
66.673	7.602	7.766	7.951	8.145
100.01	7.684	7.841	8.024	8.219
125.01	7.727	7.884	8.068	8.262
166.68	7.771	7.934	8.117	8.307
250.02	7.835	7.991	8.174	8.369
333.36	7.878	8.050	8.221	8.404
500.05	7.945	8.097	8.275	8.468
1000.1	8.017	8.186	8.361	8.545
1962.4	8.082	8.257	8.431	8.610
3428.9	8.147	8.328	8.485	8.691